ORGANIC LETTERS

2012
Vol. 14, No. 12
2964–2967

Stepwise Cyanation of Naphthalene Diimide for n-Channel Field-Effect Transistors

Jingjing Chang,[†] Qun Ye,[†] Kuo-Wei Huang,[‡] Jie Zhang,[§] Zhi-Kuan Chen,[§] Jishan Wu,[†,§] and Chunyan Chi*,[†]

*Department of Chemistry, National University of Singapore, 3 Science Drive 3, Singapore 117543, KAUST Catalysis Center and Division of Chemical and Life Sciences and Engineering, 4700 King Abdullah University of Science and Technology, Thuwal 23955-6900, Kingdom of Saudi Arabia, and Institute of Materials Research and Engineering, A*Star, 3 Research Link, Singapore 117602*

chmcc@nus.edu.sg

Received April 9, 2012

ABSTRACT

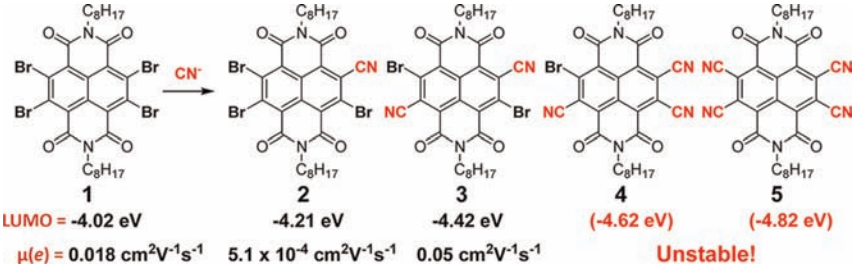

Stepwise cyanation of tetrabromonaphthalenediimide (NDI) 1 gave a series of cyanated NDIs 2−5 with the monocyanated NDI 2 and dicyanated NDI 3 isolated. The tri- and tetracyano- NDIs 4 and 5 show intrinsic instability toward moisture because of their extremely low-lying LUMO energy levels. The partially cyanated intermediates can be utilized as air-stable n-type semiconductors with OFET electron mobility up to 0.05 $cm^2 V^{-1} s^{-1}$.

Naphthalene diimide (NDI)[1] based molecules have been intensively investigated as n-type semiconductors for organic field effect transistors (OFETs). The interest stems from the early observation of the n-type behavior[1c] as well as the versatile tuning of their chemical and electronic properties by varying the substituents at the imide position[2] or on the naphthalene core.[3] In order to achieve applicable electron-transporting materials with high charge carrier mobility and good air stability, introduction of electron-withdrawing cyano groups onto the NDI framework has become an important strategy.[4]

Our interest herein is to synthesize a series of new cyanated NDI molecules such as **2**−**5** from the tetrabromo-NDI **1** (Scheme 1) and to exploit their applications as new n-type semiconductors for air-stable OFETs. The dicyanated NDI (nonbrominated analog of **3**) is known as an air-stable n-type semiconductor,[1f] while the synthesis of tetracyano NDI **5**[5] is very challenging because

[†] National University of Singapore.
[‡] King Abdullah University of Science and Technology.
[§] Institute of Materials Research and Engineering.

(1) (a) Zhan, X.; Facchetti, A.; Barlow, S.; Marks, T. J.; Rather, M. A.; Wasielewski, M. R.; Marder, S. R. *Adv. Mater.* **2011**, *33*, 268. (b) Bhosale, S. V.; Jani, C. H.; Langford, S. J. *Chem. Soc. Rev.* **2008**, *37*, 331. (c) Laquindanum, J. G.; Dodabalapur, A.; Lovinger, A. J. *J. Am. Chem. Soc.* **1996**, *118*, 11331. (d) Katz, H. E.; Johnson, J.; Lovinger, A. J.; Li, W. *J. Am. Chem. Soc.* **2000**, *122*, 7787. (e) Katz, H. E.; Lovinger, A. J.; Johnson, J.; Kloc, C.; Siegrist, T.; Li, W.; Lin, Y. Y.; Dodabalapur, A. *Nature* **2000**, *404*, 478. (f) Jones, B. A.; Facchetti, A.; Marks, T. J.; Wasielewski, M. R. *Chem. Mater.* **2007**, *19*, 2703.

(2) (a) See, K. C.; Landis, C.; Sarjeant, A.; Katz, H. E. *Chem. Mater.* **2008**, *20*, 3609. (b) Shukla, D.; Nelson, S. F.; Freeman, D. C.; Rajeswaran, M.; Ahearn, W. G.; Meyer, D. M.; Carey, J. T. *Chem. Mater.* **2008**, *20*, 7286. (c) Jung, B.; Sun, J.; Lee, T.; Sarjeant, A.; Katz, H. E. *Chem. Mater.* **2009**, *21*, 94. (d) Kantchev, E. A. B.; Tan, H. S.; Norsten, T. B.; Sullivan, M. B. *Org. Lett.* **2011**, *13*, 5432.

(3) (a) Sakai, N.; Mareda, J.; Vauthey, E.; Matile, S. *Chem. Soc. Rev.* **2010**, *46*, 4225. (b) Chopin, S.; Chaignon, F.; Blart, E.; Odobel, F. *J. Mater. Chem.* **2007**, *17*, 4139. (c) Krüger, H.; Janietz, S.; Sainova, D.; Dobreva, D.; Koch, N.; Vollmer, A. *Adv. Funct. Mater.* **2007**, *17*, 3715. (d) Suraru, S.; Würther, F. *Synthesis* **2009**, *11*, 1841.

(4) (a) Hu, Y.; Gao, X.; Di, C.; Yang, X.; Zhang, F.; Liu, Y.; Li, H.; Zhu, D. *Chem. Mater.* **2011**, *23*, 1204. (b) Gao, X.; Di, C.; Hu, Y.; Yang, X.; Fan, H.; Zhang, F.; Liu, Y.; Li, H.; Zhu, D. *J. Am. Chem. Soc.* **2010**, *132*, 3697.

10.1021/ol300914k
Published on Web 05/25/2012

Scheme 1. Synthesis of Cyanated Naphthalene Diimides **2**–**5**[a]

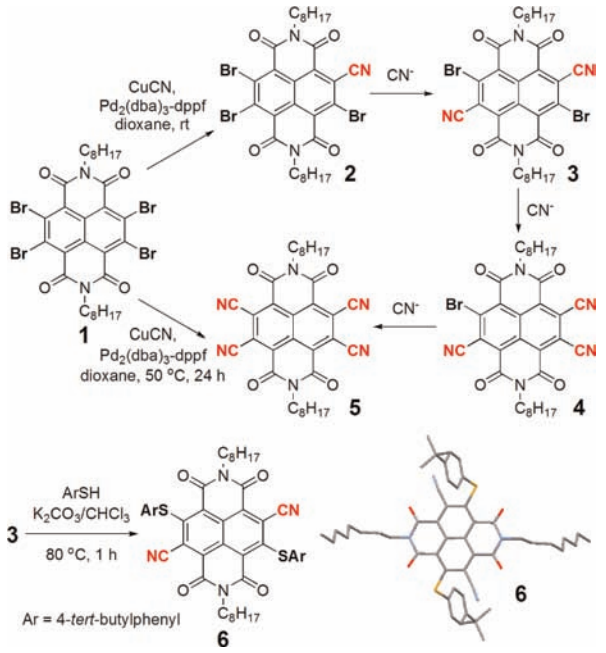

[a] Inset: single-crystal structure of **6**.

of its expected ultrahigh electron affinity. An attempted synthesis of analogues of **5** was reported.[6] However, the synthesis was not successful, and intractable results were obtained. In this work, we challenge the synthesis of **5** by a stepwise cyanation method. By studying the intermediates of this cyanation process, the synthetic problems of **5** would be better understood. The partially cyanated NDIs, however, are useful as well for air-stable n-channel OFETs.

The synthesis of the cyanated NDIs **2**–**5** is shown in Scheme 1. The cyanation of tetrabromo-NDI **1**[7] was first attempted by using CuCN/DMF/reflux protocol,[8] which was reported to be successful for cyanation of other electron-deficient systems.[1f] However, under such conditions, the reaction was plagued by severe side reactions and it generated a mixture of intractable products which are difficult to identify. We then attempted the palladium-catalyzed cyanation protocol[9] which could be carried out under milder conditions. The cyanation of **1** was successfully carried out with $Pd_2(dba)_3$ as Pd source, 1,1′-bis-(diphenylphosphino)ferrocene (dppf) as ligand, CuCN as cyanide source, and dioxane as solvent. The amount of catalyst and ligand as well as the reaction temperature had to be carefully controlled. The amount of palladium catalyst had to be less than 0.03 equiv per bromine and the amount of ligand less than 0.06 equiv per bromine. Otherwise, phosphonium salt formation would be observed as the major side reaction, especially at elevated temperatures.[10] By setting the reaction temperature at 50 °C, the tetracyanated product **5** was obtained after 24 h, and its presence was confirmed by MALDI-TOF MS analysis of the reaction solution (Figure S1 in the Supporting Information). However, it was sensitive to moisture and silica gel, which made the purification unsuccessful. The decomposition products of **5** in air were analyzed by MALDI-TOF MS (Figure S1, Supporting Information), and it was found that hydrolysis happened with **5**, most probably on the cyano groups. This side reaction would be caused by the low-lying LUMO of **5**, which made it vulnerable to be attacked even by weak nucleophiles such as water.

In order to probe this stability issue, we then carried out a stepwise cyanation on **1** by running the reaction at room temperature. All cyanated compounds **2**–**5** were detected during the reaction by MALDI-TOF mass spectrometry as shown in Figure 1. The monocyanated and dicyanated naphthalene diimides **2** and **3** as major products were successfully separated in 64% and 61% yield by column chromatography after reaction for 8 and 16 h, respectively. After 48 h, almost only the tetracyano-NDI **5** was detected. However, **4** and **5** could not be separated because of quick decomposition upon contact with moisture or silica gel. Interestingly, for the dicyanated compound, only one isomer was found even though three isomers should be theoretically possible. The structure of **3** was unambiguously confirmed by the single-crystal structural analysis of compound **6**, which was prepared by nucleophilic attack of the two bromines on **3** by 4-*tert*-butylthiophenol (Scheme 1). This unexpected regioselectivity could be ascribed to two reasons: first, the second cyanation was directed by the electron-withdrawing effect of the first cyano group, and second, the reaction was conducted at room temperature

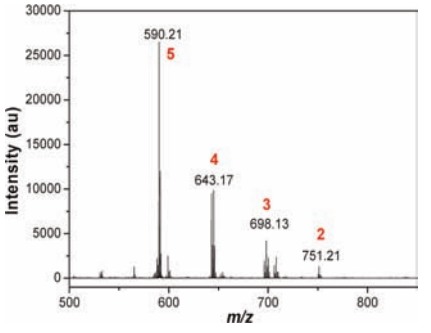

Figure 1. MALDI-TOF mass spectrum of the reaction mixture after reaction at room temperature for 24 h.

(5) Könemann, M. Naphthalenetetracarboxylic Acid Derivatives and Their Use As Semiconductors. WO/2007/074137.

(6) Dawson, R. E.; Hennig, A.; Weimann, D. P.; Emery, D.; Ravikumar, V.; Montenegro, J.; Takeuchi, T.; Gabutti, S.; Mayor, M.; Mareda, J.; Schalley, C. A.; Matile, S. *Nat. Chem.* **2010**, *2*, 533.

(7) (a) Röger, C.; Würthner, F. *J. Org. Chem.* **2007**, *72*, 8070. (b) Gao, X.; Qiu, W.; Yang, X.; Liu, Y.; Wang, Y.; Zhang, H.; Qi, T.; Liu, Y.; Lu, K.; Du, C.; Shuai, Z.; Yu, G.; Zhu, D. *Org. Lett.* **2007**, *9*, 3917.

(8) Ellis, G. P.; Romney-Alexander, T. M. *Chem. Rev.* **1987**, *87*, 779.

(9) Qu, H.; Cui, W.; Li, J.; Shao, J.; Chi, C. *Org. Lett.* **2011**, *13*, 924.

(10) Ye, Q.; Chang, J.; Huang, K. W.; Chi, C. *Org. Lett.* **2011**, *13*, 5960.

with a slow rate, and hence, the thermodynamically controlled cyanation would occur at sites with least steric hindrance.

The electrochemical properties of **1**–**3** were investigated by cyclic voltammetry and differential pulse voltammetry (Figure 2a and Figure S2, Supporting Information). Compound **2** exhibited two reversible reduction waves with half-wave potential $E_{1/2}^{red}$ at −0.66 and −1.11 V (vs Fc^+/Fc). Compound **3** showed two similar reversible reduction waves with $E_{1/2}^{red}$ at −0.45 and −1.00 V, and one quasi-reversible reduction wave with $E_{1/2}^{red}$ at −1.56 V. Compound **1** showed three quasi-reversible reduction waves with $E_{1/2}^{red}$ at −0.89, −1.26, and −1.48 V. The LUMO energy levels of **1**, **2**, and **3** were estimated to be −4.02, −4.21, and −4.42 eV, respectively, based on the onset potential of the first reduction wave. It was worthy to note that after replacement of one bromine atom with a cyano group, the LUMO energy level was reduced by ca. 0.2 eV, showing a good linear relationship with the number of CN groups (Figure 2b). DFT (B3LYP/6-31G*) calculations predicted that the LUMO energy levels of **1**–**5** are −3.69, −3.95, −4.28, −4.54, and −4.82 eV (Figure S3, Supporting Information), which also exhibit a good linear relationship with the number of CN groups (Figure 2b). Thus, it is reasonable to make a linear extrapolation of the experimental plot and the LUMO energy levels of **4** and **5** are estimated to be −4.62 and −4.82 eV, respectively. The very low lying LUMO energy levels reflected the highly electron-deficient nature of **4** and **5**, which would be the most possible origin of their instability.

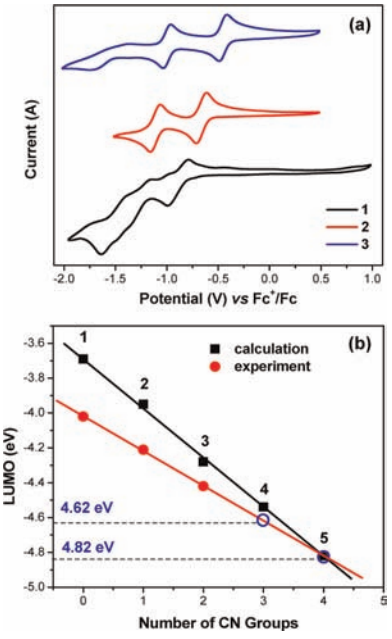

Figure 2. (a) Cyclic voltammograms of **1**–**3** measured in dry CH_2Cl_2. (b) Plots of the calculated (DFT at B3LYP/6-31G* level) and experimental LUMO energy levels of **1**–**5** with the number of CN groups.

Solutions of **1**–**3** in chloroform show well-resolved absorption bands at 300–460 nm, with only a slight shift of the wavelength upon cyanation (Figure S4, Supporting Information). The optical energy gaps of **1**–**3** estimated from the absorption onset at the longest wavelength are nearly the same, i.e., 2.77 eV. Compound **6** shows an entirely different absorption spectrum, with a large broad absorption peak at 620 nm that was believed due to the intramolecular charge transfer.

Field effect transistors with **1**–**3** as active compounds were fabricated in a bottom-gate, top-contact configuration (see details in the Supporting Information). A thin film of semiconductor materials was deposited at different substrate temperature T_d by vapor deposition onto a p+-Si wafer with 200 nm of thermally grown SiO_2 as the dielectric layer. The SiO_2 substrate was modified by either octadecyltrimethoxysilane (OTMS) or CYTOP (poly(perfluorobutenylvinylether)) amorphous fluoropolymer or without any modification. The typical transfer and output curves measured in N_2 on OTMS-modified substrate with T_d = 60 °C are shown in Figure 3, and the device characteristics data at various T_d temperatures are collected in Table 1. All of the devices exhibit typical n-channel behavior, and the highest FET electron mobility measured in N_2 is 0.018, 5.1×10^{-4}, and 0.050 $cm^2\ V^{-1}\ s^{-1}$ for **1**, **2**, and **3**, respectively. The electron mobilities are dependent on T_d and dielectric surface treatment. For example, the mobility of **3** increased from 0.018 $cm^2\ V^{-1}\ s^{-1}$ at rt to 0.050 $cm^2\ V^{-1}\ s^{-1}$ for thin film deposited at 100 °C. The thin film on $OTMS/SiO_2$ exhibited higher performance (0.050 $cm^2\ V^{-1}\ s^{-1}$) compared to bare SiO_2 substrates which only gave a low mobility of 2.4×10^{-5} $cm^2\ V^{-1}\ s^{-1}$. The threshold voltage (V_{th}) shifts to more negative with increasing the number of cyano groups from **1** to **2** and to **3**, indicating the higher the electron affinity the easier it is to create mobile electrons at low gate bias.

Thin films of **1**–**3** deposited at different T_d exhibited a similar X-ray diffraction pattern which can be correlated to a lamellar packing mode (Figure S5–7, Supporting Information) with a $d_{(001)}$ spacing of 17.0, 18.4, and 18.5 Å, respectively. Thin film of **2** showed less intense and broader diffraction peaks compared with **1** and **3**, indicating a less ordered microstructure. AFM images revealed highly crystalline surface microstructure and the crystallite size tended to increase with increasing T_d for all compounds (Figure S8–10, Supporting Information), which can explain the higher mobility at the higher substrate temperature due to minimized grain boundaries. A thin film of **2** exhibited smaller grains and much more grain boundaries, which limit the efficient charge transport and correspond to lower charge carrier mobility.

The OFET devices operated in ambient conditions showed different degradation (Table S1, Supporting Information). Compound **1** with the lowest electron-affinity exhibited the largest device variations (~1000×), while **3** with the highest electron-affinity showed a smaller decrease in charge carrier mobility by a factor of ~10×. This trend gave a

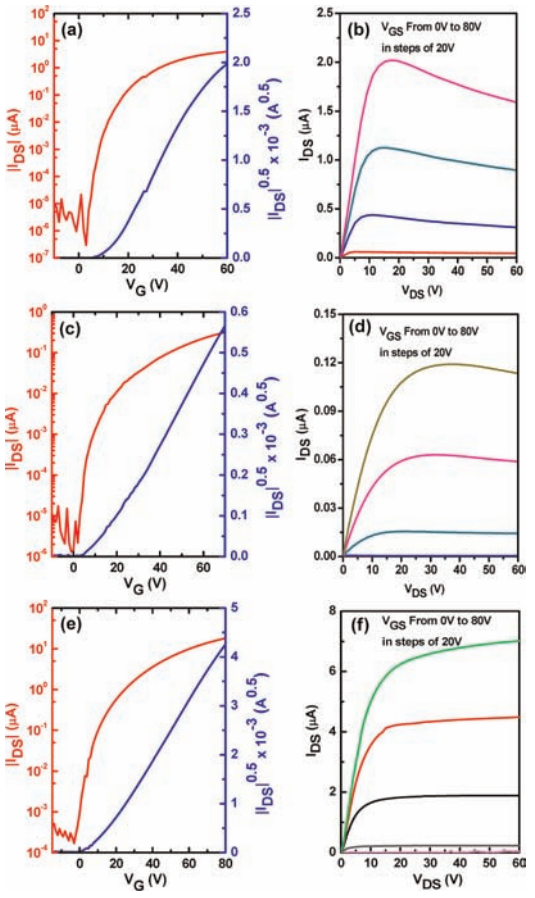

Figure 3. Representative OFET transfer and output characteristics of **1** (a, b), **2**(c, d), and **3** (e, f) thin films (T_d = 60 °C) on OTMS-modified substrates in N_2.

Table 1. OFET Characteristics for **1**–**3** Measured in N_2 on OTMS-Modified Substrates

	T_d (°C)	μ (*e*) [$cm^2\ V^{-1}\ s^{-1}$]	V_T [V]	on/off
1	rt	0.011	19–24	10^6
	60	0.018	15–20	10^6
	100	0.012	14–19	10^5
2	rt	3.7×10^{-4}	12–18	10^5
	60	3.9×10^{-4}	13–17	10^5
	100	5.1×10^{-4}	12–17	10^5
3	rt	0.018	3–6	10^5
	60	0.036	3–7	10^5
	100	0.050	4–7	10^4

sign that the n-type ambient sensitivity could be decreased with increasing of electron affinity. The V_{th} of **1** was significantly shifted to positive with about 15–30 V due to electron traps at the interface between the semiconductor and dielectric. However, the V_{th} of **2** and **3** were both slightly shifted to negative voltage maybe due to unintentional doping by electron-rich chemical functionalities and/or the local electric field.[11] The electron trap sites like silanol groups on SiO_2 could be neglected when the LUMO of semiconductor is lower than −3.8 eV,[12] which may also explain the good device stability of **2** and **3**.

OFETs on CYTOP/SiO_2 bilayer substrates showed comparable performance to that on OTMS-modified substrates, showing the highest electron mobilities of 0.017, 5.1×10^{-4}, and 0.047 $cm^2\ V^{-1}\ s^{-1}$ for **1**, **2**, and **3**, respectively, when measured in N_2 (Figure S11 and Table S2, Supporting Information). The OFET devices also gave a more positive V_{th} and a larger I_{on}/I_{off} ratio. When the devices were operated in ambient conditions, the mobility showed a smaller decrease (~2×). Thin films of **1**–**3** deposited on CYTOP/SiO_2 exhibited similar XRD pattern but with enhanced reflection intensity (Figure S12–14, Supporting Information) compared to the OTMS/SiO_2 substrate, indicating more ordered packing. The surface morphology also changes slightly (Figure S15–17, Supporting Information). Solution-processed OFET devices were fabricated by spin-coating **3** in chloroform onto OTMS/SiO_2 substrate, and the device showed an average FET electron mobility of 0.02 $cm^2\ V^{-1}\ s^{-1}$ with good air stability (Figure S18–20, Supporting Information), which is comparable to vapor deposited devices.

In summary, stepwise cyanation of tetrabromonaphthalene diimide **1** gave a series of cyanated compounds **2**–**5**. The electron affinity showed a good linear relationship with the number of the cyano groups and the extremely low-lying LUMO energy level of **4** and **5**, making them unstable to moisture. The mono- and dicyanated NDIs **2** and **3**, however, can be obtained as stable n-type semiconductors and used for air-stable n-channel OFETs with moderate electron mobilities. This research implies that in the search for new high-performance n-type semiconductors we need to find a good balance between the materials' stability and device stability by careful control of the electron affinity.[13]

Acknowledgment. C.C. acknowledges financial support from the National University of Singapore start-up grant R-143-000-486-133 and MOE AcRF FRC grant R-143-000-444-112. K.-W.H. acknowledges financial support from KAUST. We thank Dr. Tan Geok Kheng at NUS for crystallographic analysis.

Supporting Information Available. Synthetic procedures and characterization data. Crystallographic data of compound **6**. Electrochemical data. DFT calculation data. Details of FET fabrication and characterizations. This material is free of charge via Internet at http://pubs.acs.org.

(11) (a) Bao, Z.; Lovinger, A. J.; Brown, J. *J. Am. Chem. Soc.* **1998**, *120*, 207. (b) Jones, B. A.; Ahrens, M. J.; Yoon, M.-H.; Facchetti, A.; Marks, T. J.; Wasielewski, M. R. *Angew. Chem., Int. Ed.* **2004**, *43*, 6363.

(12) Yoon, M.-H.; Kim, C.; Facchetti, A.; Marks, T. J. *J. Am. Chem. Soc.* **2006**, *128*, 12851.

(13) Jones, B. A.; Facchetti, A.; Wasielewski, M. R.; Marks, T. J. *J. Am. Chem. Soc.* **2007**, *129*, 15259.

The authors declare no competing financial interest.